◆ Human Brain Mapping 38:53–67 (2017) ◆

Decreased Between-Hemisphere Connectivity Strength and Network Efficiency in Geriatric Depression

Xuesong Li,[1] David C. Steffens,[2] Guy G. Potter,[3] Hua Guo,[1] Sen Song,[1] and Lihong Wang[2,3]*

[1]*Department of Biomedical Engineering, School of Medicine, Tsinghua University, Beijing, China*
[2]*Department of Psychiatry, University of Connecticut School of Medicine, Farmington, Connecticut*
[3]*Department of Psychiatry and Behavioral Science, Duke University, Durham, North Carolina*

Abstract: White matter (WM) lesions have been recognized as a key etiological factor in geriatric depression. However, little is known about the topological pattern changes of WM in geriatric depression in the remitted state (RGD) and its relationship to depressive episodes. To address these questions, we acquired diffusion tensor images in 24 RGD and 24 healthy participants. Among them, 10 patients and 19 healthy controls completed a 1-year follow up. Between-hemisphere connectivity and graph theoretical methods were used to analyze the data. We found significantly reduced WM connectivity between the left and right hemisphere in the RGD group compared with the control group. Those with multiple depression episodes had greater reduction in between-hemisphere connectivity strength than those with fewer episodes. In addition, the RGD group had a reduced global clustering coefficient, global efficiency, and network strength, and an increased shortest path length compared with the controls. A lower clustering coefficient was correlated with poorer memory function. The reduction of nodal clustering coefficient, global efficiency, and network strength in several regions were associated with slower information processing speed. At 1-year follow up, the network properties in the RGD subjects were significantly changed suggesting instability of WM network properties of depressed patients. Together, our study provides direct evidence of reduced between-hemisphere WM connectivity with greater depressive episodes, and of alterations of network properties with cognitive dysfunction in geriatric depression. *Hum Brain Mapp 38:53–67, 2017.*

Key words: between-hemisphere connectivity; graph theory; geriatric depression; diffusion tensor imaging; depression episodes; cognitive function

Contract grant sponsor: Paul B. Beeson Patient-Oriented Research Career Development Award in Aging; Contract grant number: K23-AG028982 (LW); Contract grant sponsor: NIMH; Contract grant number: R01MH098301-01A1 (LW, GP and DS); Contract grant sponsor: NIMH Career Development Award; Contract grant number: K23 MH087741 (GP).

*Correspondence to: Lihong Wang, MD, PhD; Department of Psychiatry, University of Connecticut School of Medicine, 263 Farmington Ave, Farmington, CT, 06030. E-mail: lwang@uchc.edu

Received for publication 9 May 2016; Accepted 29 July 2016.
DOI: 10.1002/hbm.23343
Published online 9 August 2016 in Wiley Online Library (wileyonlinelibrary.com).

INTRODUCTION

Different from depression in younger adults, geriatric depression often occurs in individuals with cerebrovascular disease, particularly in those with white matter hyperintensities (WMHs) seen in magnetic resonance imaging (MRI) brain scans [Alexopoulos et al., 1997]. While white matter damages in major depression in younger adults are still under debate [Choi et al., 2014], increased burden of WMHs in geriatric depression has been consistently found. WMHs have been shown to negatively impact both mood and cognition [Alexopoulos et al., 2002]. Sheline and colleagues reported a strong correlation of WMH burden in bilateral superior longitudinal fasciculus and left uncinate fasciculus with executive dysfunction and memory impairment [Sheline et al., 2008]. Examining fractional anisotropy (FA), a measure of white matter integrity from diffusion tensor imaging (DTI) data, Murphy and colleagues demonstrated a correlation of FA value of the frontostriatal-limbic regions (including white matter lateral to the anterior and posterior cingulate cortex, prefrontal, insular, and parahippocampal regions) with executive function as measured by the Stroop color-word interference task [Murphy et al., 2007]. In addition, Dalby and colleagues reported that reduced FA in the left superior longitudinal fasciculus and the right uncinate fasciculus in geriatric depression was significantly correlated with depression severity [Dalby et al., 2010]. Supporting these findings, ours and others' studies have indicated that deficits in the uncinate fasciculus could induce depressive symptoms and cognitive dysfunction through interfering functional connectivity between the ventromedial prefrontal (vmPFC) and amygdala as well as between the vmPFC and caudate [Steffens et al., 2011]. Evidence from these and other studies led to the "disconnection theory" of geriatric depression proposed by Taylor and colleagues [Taylor, 2013]. Given the increasing view of major depression as a network-based disorder involving multiple neural circuits [Drevets et al., 2008; Mayberg, 2009], it is important to investigate how disconnections of white matter networks at the global and local level impact on depressive symptoms and cognitive dysfunction.

With significant advances in neuroimaging technology in recent years, several data analytic methods have been developed in assessing network connectivity, including between-hemisphere connectivity, network-based statistics, and graph theoretical analysis. Between-hemisphere connectivity analysis can be used to assess the strength of the connections between left and right symmetrical regions. This is an important measure in major depression given the well-known frontal asymmetry theory of depression [Davidson, 1993; Sackeim et al., 1982]. In major depression, hypometabolism/hypoactivation in the left dorsolateral prefrontal cortex (DLPFC) and hypermetabolism/hyperactivation in the right DLPFC have been frequently reported [Davidson et al., 2003; Elliott et al., 2002; Grimm et al., 2008; Keedwell et al., 2005; Mayberg, 2003; Phillips, 2003]. Although left and right frontal activity asymmetry is important to the therapeutic effect of antidepressants [Wang et al., 2015] and repetitive transcranial magnetic stimulation in MDD [Bermpohl et al., 2006; Maeda et al., 2000; Wei et al., 2014], few have examined whether the frontal asymmetry activity in MDD is related to the white matter disconnection. We speculated that there might be white matter disconnections between the left and right hemispheres which are related to frontal asymmetric function and depression symptoms.

Network-based statistics (NBS) has been developed to assess connectivity strength at a network level and control for multiple comparisons [Zalesky et al., 2010a]. This technique is powerful in identifying weakened connections in some subnetworks. NBS analysis is often followed by graph theoretical analysis. Graph theoretical analysis has been increasingly used to evaluate the global and local network properties [Boccaletti et al., 2006; Bullmore and Sporns, 2009; Cohen et al., 2008; Johansen-Berg et al., 2004]. The graph approach "enables assessment of both the efficiency of information transfer between different brain regions and the implications of widespread damage or local damage to specific anatomic regions" [Petrella, 2011]. Abnormal topological connections in schizophrenia, Alzheimer's disease, aging, and multiple sclerosis have been reported [Brown et al., 2013; Gong et al., 2009b; He et al., 2008; Lo et al., 2010; Shu et al., 2011; Zalesky et al., 2011] based on graph theoretical analyses. To our knowledge, there is only one report in geriatric depression in the literature using graph theoretical analyses on white matter connectivity [Bai et al., 2012]. Here, the authors compared geriatric depression patients who remitted from depression symptoms (RGD) with amnestic mild cognitive impairment patients (aMCI) as well as healthy controls, and found significantly decreased network strength and global clustering efficiency, as well as increased absolute path length in both RGD and aMCI in comparison with healthy controls. This study indicates that microdamages in white matter can impact on network connectivity efficiency. However, the study did not report any correlation between the white matter network properties with depressive symptoms or cognitive function. Given that WMH has been viewed as a vulnerable factor to geriatric depression, it is important to further confirm the existence of changes of white-matter network properties in geriatric depression even at remitted state, whether the alterations are stable over time, whether they are related to accumulation of depressive episodes or are a predispositional factors to future new depressive episodes and/or future cognitive decline. So far, there are no longitudinal studies in the literature that examined the changes of white matter network properties in geriatric depression over time or in relationships with depressive episodes.

In this study, we used diffusion tensor imaging (DTI) probabilistic tractography [Basser et al., 2000] to investigate the topological organization of whole-brain WM networks in older adults remitted from depression (remitted geriatric depression, RGD). We investigated the connectivity between the left and right hemisphere, NBS, and the white matter network properties to investigate which of

TABLE I. Demographic and neuropsychological data

	RGD ($n = 24$) Mean(SD)	HC ($n = 24$) Mean(SD)	P value	Number of missing data
Age	69.67 (6.98)	73.5 (8.58)	0.096	
Education	15.21 (3.04)	15.75 (2.51)	0.504	
Gender	11F/13M	15F/9M	0.247	
MARDS	2.58 (2.99)	0.67 (1.17)	0.0053*	
Cognitive Function				
Information Speed	0.37 (0.84)	0.69 (0.82)	0.189	
Memory	0.20 (0.96)	0.28 (0.80)	0.774	
Executive Function	0.08 (0.87)	0.14 (0.70)	0.783	HC:1
Total Score(average of I,M,E)	0.22 (0.74)	0.45 (0.55)	0.22	HC:1

All variables were compared between groups using two-sample t test except gender, which was examined using chi-square test. *$P < 0.05$ MARDS, Montgomery–Asberg Depression Rating Scale; RGD, remitted geriatric depression; HC, healthy control.

these measures are associated with depression symptoms or cognitive function. We also aimed to examine whether more severe white matter damages are related to more depressive episodes or greater chance of developing a new depression episode over a 1-year follow up. We hypothesized that the property measures of regional white matter connectivity would have stronger correlation with depressive symptoms and with cognitive dysfunction. A different dataset was also analyzed to replicate the findings.

MATERIALS AND METHODS

Participants

Twenty four older patients (11 female, mean age ± SD = 69.67 ± 6.98 years) who were diagnosed with a major depression episode and twenty four older healthy controls (15 female, mean age ± SD 73.5 ± 8.58 years) were recruited from the National Institute of Mental Health-supported Neurocognitive Outcomes of Depression in the Elderly (NCODE) study at Duke University. Eligibility for the study was based on initial self-report measures, cognitive screening tools, and medical examinations. Specifically, participants underwent complete standardized clinical assessments using Duke Depression Evaluation Schedule (DDES) [Robins et al., 1981]. For healthy participants, the Center for Epidemiologic Studies Depression Scale (CES-D) was used to screen for current depressive symptoms (with a cutoff score of 16). The DDES was followed by a standard clinical assessment by study psychiatrists. A clinician-rated measure of current depression severity (Montgomery-Asberg Depression Rating Scale, MADRS) was completed. Only depressed patients who had MADRS scores below 8 for at least 2 months were considered as remitted and were included in the RGD group. Exclusion criteria for depressed subjects included: (1) another major psychiatric illness, including bipolar disorder, schizophrenia, or dementia; (2) alcohol or drug abuse or dependence; (3) neurological illness, including dementia, stroke, and epilepsy; (4) medical illness, medication use, or disability that would prevent the participant from completing neuropsychological testing; and (5) contraindications to MRI. All non-depressed subjects were cognitively intact, had no history or clinical evidence of dementia, and all scored 28 or more on the Mini-Mental State Examination (MMSE). Among the RGD participants, 6 were receiving antidepressant monotherapy (3 on an SSRI, 2 on venlafaxine, and 1 on amitriptyline), and 5 were receiving combination treatment [4 on Selective serotonin reuptake inhibitor (SSRI) combined with either Serotonin–norepinephrine reuptake inhibitor (SNRI), Serotonin antagonist and reuptake inhibitor (SARI), or Norepinephrine-Dopamine Reuptake Inhibitor (DNRI) and 1 on SSRI, NDRI, and SNRI]. The clinical profiles of these subjects are summarized in Table I.

The study received ethics committee approval by the Duke School of Medicine Institutional Review Board and, after being explained the purpose and procedures to be used in the study, all subjects provided written informed consent.

To investigate how the white matter network changes over time, we further followed these subjects for a year. Ten out of the twenty-four RGD and nineteen out of the twenty-four healthy control subjects completed 1-year follow-up examinations (including clinical evaluations, neuropsychological tests, and the DTI scans). Among the 10 RGD subjects, three had a new depressive episode within the 1-year follow up.

Neuropsychological Measures

Subjects' cognitive function was assessed using a short, 30-minute battery of neuropsychological tests prior to DTI scans. The neuropsychological battery consisted of Mini-Mental State Exam (MMSE), Category Fluency (Vegetable Naming), Hopkins Verbal Learning Test-Revised (HVLT-R), Immediate and Delayed Story Recall from the Rivermead Behavioral Memory Test, Trail Making Test (Trail A and Trail B), WAIS-III Digit Span, WAIS-III Digit–Symbol Substitution Test (DSST), and Stroop Color and Word Test (Stroop). The mean and standard deviation of the healthy control group on each measure were used to calculate z scores for each subject. We further subgrouped the tests in three cognitive domains with the averaged z score of the

Trail B and the Stroop interference tests as a measure for executive function, the averaged z score of the Rivermead immediate and delay Story Recall, and the HVLT-R Immediate and Delayed Story Recall as a measure for memory, and the averaged z score of the digit span and DSST as a measure for information processing speed.

Images Acquisition

Data acquisition was performed using a 3.0-Tesla GE Signa EXCITE scanner from Duke-UNC Brain Imaging and Analysis Center with the following parameters: $b_0 = 1{,}000$ s/mm^2, flip angle = 90°, TR/TE = 17,000 ms/78 ms, imaging matrix = 128 × 128, FOV = 256 × 256 mm^2, 72 contiguous slices, resulting in a voxel dimension of 2 × 2 × 2 mm^3 reconstructed resolution. A total of 25-direction images were acquired. A high-resolution T1-weighted SPGR structural images in coronel view were acquired with slice thickness of 1 mm without a gap: TR/TE =7.46 ms/2.98 ms, FOV = 256 × 256 mm^2 (matrix = 256 × 256 × 216).

Data Preprocessing

The data analyses consisted of three major steps: (1) data preprocessing, (2) probabilistic fiber tractography and network construction, and (3) network analyses. We performed the data preprocessing and fiber tractography using the FMRIB's Diffusion Toolbox (http://fsl.fmrib.ox.ac.uk/fsl/fslwiki/FDT). The data preprocessing included eddy current and motion artifact correction, and co-registration. Eddy current distortions and motion artifacts were corrected by applying affine alignment of each diffusion-weighted image to the b_0 image. After this process, the tensor elements were estimated and then the reconstructed tensor matrix was diagonalized to obtain three eigenvalues and eigenvectors [Behrens et al., 2003]. The probabilistic distribution of fiber orientations for each voxel was estimated with a two-tensor model following the instruction of the BEDPOSTX (Bayesian Estimation of Diffusion Parameters Obtained using Sampling Techniques with modeling crossing fibers within each voxel) program on FSL website [Smith et al., 2004] (http://fsl.fmrib.ox.ac.uk/fsl/fslwiki/FDT/UserGuide).

Network Construction

The construction of a brain network critically depends on the nodes and edges. Many studies used nodes from the automatic anatomical labeling (AAL) scheme [Tzourio-Mazoyer et al., 2002] which includes 90 cortical and subcortical regions, 45 for each hemisphere [Cao et al., 2013; Gong et al., 2009a]. The label for each region is listed in the Supporting Information Table 1. Others defined nodes in a high resolution (a finer scale), that is, either voxel-based or small volume-based nodes. In our study, we used the AAL labeling system to define the 90 nodes, and we reported our results mainly based on this low resolution analyses and reported the higher spatial resolution results using the small volume-based method in Supporting Information. Below is a brief introduction of the procedures for network constructions.

Network nodes

First, individual b_0 images were co-registered to T1-weighted images, and the transformed T1 images were then linearly transformed to the ICBM 152 T1 template in the MNI space (Fig. 1A). Using this procedure, we obtained the 45 regions from each hemisphere, each region representing a node of the network, which resulted in a symmetric atlas-based 90 × 90 matrix. For the high-resolution network construction, each of the 90 regions was then subdivided into small ROIs using k-means cluster subdividing method, which resulted in 1112 regions in total [Cao et al., 2013; Hagmann et al., 2007, 2008; Yap et al., 2010; Zalesky et al., 2010b]. After the regions were defined, all of the subsequent procedures for the high-resolution network analyses were similar to the low-resolution network analyses which would not be repeated here.

Network edges

As mentioned earlier, to reconstruct the whole-brain WM tract matrix, we performed probabilistic tractography using the FSL Diffusion Toolbox (FSL, version 5.01), and sampled 5,000 streamline fibers per voxel. For each sampled fiber, a sample direction was first drawn from the local direction distribution at the seed voxel, then the probability tract was calculated every 0.5mm from the sample direction to a new position, and finally, a new sample direction from the local distribution was obtain at this new position. Using the atlas-defined nodes as seed regions, the connectivity probability to each of the rest of the regions (the other 89 regions for the low-resolution analysis) was calculated separately. The connectivity probability between regions was defined as the weight of network edge. To define the network edges, we computed $w(i,j)$ as the weight between brain region i and j, for each subject, and a 90 × 90 symmetric weighted network matrix was constructed separately (Fig. 1B). To remove spurious connections, only those connections existing in more than 80% of subjects in the group were included in the network construction.

Network Analysis

For the weighted WM networks, we calculated both global and regional network properties. The global properties included: global shortest path length (Lp), global clustering coefficient (Cp), global fault tolerant efficiency (also known as local efficiency, LocE), global efficiency (gE), and global network strength (NS). The regional network metrics included: nodal shortest path length, nodal clustering coefficient, nodal efficiency, nodal fault tolerant efficiency, and nodal network strength [Iturria-Medina et al., 2007, 2008; Latora

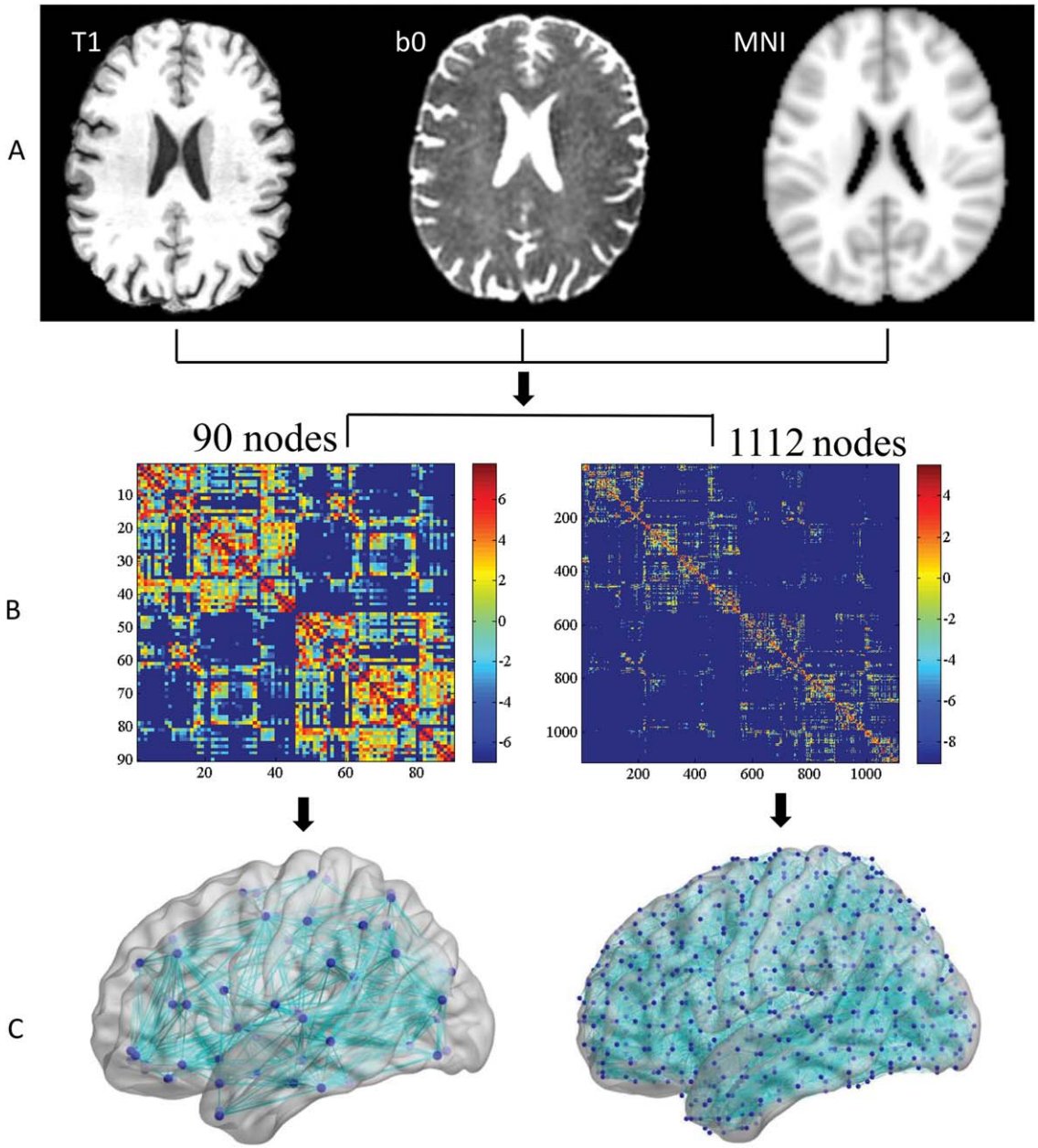

Figure 1.

Flowchart for the construction of the white matter (WM) structural network. **A**, calculate transformation matrices among T1, DTI, b0, and MNI standard brain; **B**, use the probabilistic fiber tracking method to generate fiber topography and create individual structural connectivity matrix based on 90 nodes (low resolution) and 1,112 nodes (high resolution). The sparsity are 49.6% for low resolution and 9.12% for high-resolution; **C,** construct the resultant WM networks in the MNI standard space (The nodes and edges were visualized by BrainNet Viewer software, http://www.nitrc.org/projects/bnv/). [Color figure can be viewed at wileyonline library.com.]

and Marchiori, 2001; Watts and Strogatz, 1998]. All network analyses were calculated using the GRETNA (http://www.nitrc.org/projects/gretna/) software.

Global efficiency

The global efficiency of a *node* was computed by adding all of the connection efficiency of node i to all of the other

nodes. $E_{node}(i)=\frac{1}{N-1}\sum_{j\neq i\in G}\frac{1}{L_{ij}}$ *Global* efficiency of the global network was the average of all of the nodal efficiency. Higher value means more efficient for information transfer through the whole brain.

Fault tolerant efficiency (local efficiency)

For a node i, the *nodal* fault tolerant efficiency $E_{glob}(G_i)$ represents how much the network is fault tolerant when the node i and its edges are removed. It reflects how stable and how efficient the network is for information transfer from node i to all regions node i connects with. *Global* fault tolerant efficiency is an average of the nodal fault tolerant efficiency of all nodes. A bigger value means high fault tolerant efficiency for information transfer across the whole brain. $E_{loc}(G)=\frac{1}{N}\sum_{i\in G}E_{glob}(G_i)$

Clustering coefficient

Nodal clustering coefficient represents the likelihood of node i and its neighbor's connection $CC_i=\frac{1}{k_i(k_i-1)}\sum_{j,k\in G}(w_{i,j}w_{j,k}w_{k,i})$. The w_{ij} is the connection weight from node i to node j, k_i is the degree of the node i. Higher nodal CC value means strong connectivity with the neighbor connection. *Global clustering coefficient* was the average of all nodal clustering coefficient. A higher value means higher clustering coefficient connection within the whole network.

Network strength

For a node i, the *nodal* network strength *G* was computed by sum of the edge weights w_{ij} linking to node i. The greater value means more connection strength from the node i to its neighbor nodes. $S_i=\sum_{j\in G}w_{ij}$ *Global network strength* is the average of the strengths across all of the nodes in the network. The bigger value means heavily connection strength in the whole network. $S=\frac{1}{N}\sum_{i\in G}S_i$

Shortest path length

The shortest path length of a *node* L_{ij} was defined as the length of path between node i and node j with the shortest length. The nodal shortest path length was computed by adding all the shortest path of a node i to all of the other nodes. *Global* shortest path length is the average of all of the nodal shortest path length, smaller value means fast speed information transfer to the whole brain. $L_p=\frac{1}{N(N-1)}\sum_{i\neq j\in G}L_{ij}$

Hubs

Node i was considered to be a hub if its nodal *efficiency* was at least 1 SD greater than the averaged nodal efficiency of the network (i.e., $E_{node}(i)>\text{mean}+\text{SD}$), meaning it was a key region for information transfer.

Statistical Analysis

To examine group difference in the demographic and neuropsychological data, two sample t tests for the continuous variables were conducted. A Chi square test was conducted for the binary variables. The significant level was set at $P<0.05$ for both type of tests.

To determine the significant level of difference in the between-hemisphere connectivity between the RGD and control groups, we compared the numbers of significant connections between the two hemispheres between the RGD and control groups using permutation test. For each permutation, all of the subjects were randomly reallocated into two groups and did the statistical comparison. The same procedures were repeated 5,000 times (5,000 permutations).

To determine the significance level of the alternated connectivity subnetworks in the RGD group relative to the control group, we used the NBS method following Zalesky and colleagues [Li et al., 2014; Zalesky et al., 2010a]. Briefly, first, we made a mask which included voxels that either the patient group or control group had 80% fibers. Then, a two sample one-tail *t*-test was computed on each connection link within the mask. The significant threshold was set at *P* value <0.05. To correct for multiple comparison, a nonparametric permutation test (5,000 permutations) was used. Those connection of each component based on those connection links was recorded. The maximally connected component size was identified. Finally, for a connected component of size M found in the correct grouping of controls and patients, the corrected p value was determined by finding the proportion of the 5,000 permutations for which the maximally connected component was larger than M.

To examine group difference in network properties, two-sample *t* tests were conducted for both global and regional parameters as listed above. The significance level was set at $q<0.05$ using false discovery rate (FDR) correction for multiple comparisons. We also examined the difference between RGD and health controls in changes of each global and regional network property over the 1 year (year 1–year 0) using two sample *t* tests (see Supporting Information for detailed descriptions of analyses and results).

To further investigate the association between the network properties and depression symptoms as well as cognitive dysfunction, Pearson correlation coefficient analyses were conducted on those network properties that showed significant differences between the patient and control groups during the baseline period. Depression severity was measured using MADRS, and the cognitive function was measured using the mean Z score of each neuropsychological battery measure as mentioned earlier, using the results from our control subjects to calculate the standardized score as a norm. The correlations between the subdomains of cognitive function including executive function, memory, and information processing speed with network properties were also computed. All analyses were corrected for multiple comparisons using FDR correction with $q<0.05$.

To study whether accumulated depressive episodes are associated with white matter network properties or not, we tracked the number of depressive episodes from the time of first diagnosis of major depression up to the time of study enrollment. We also examined whether white matter damage was a vulnerability factor for future depression episodes. Given that 1 year might be too short to develop a new depressive episode, we examined the correlation between the baseline network properties with the greatest increase of MADRS during the 1-year period by using the highest MADRS during the 1-year period minus baseline MADRS. The significance level for all correlation analysis was set at $P < 0.05$.

Data Replication

Since there is high fiber intensity in and around the corpus callosum, our DTI data with only 25 directions may not be sufficient enough to properly reflect the between-hemisphere connectivity. To validate our results in the main study, we analyzed the between-hemisphere connectivity on a different dataset which had 128 directions. This dataset was from 30 currently depressed patients [19 Females, 11 males, mean age (SD) = 71.7 (7.45) years] and 28 health control participants [19 Females, 9 males, mean age (SD) = 75.9 (6.94) years]. All patients were not under any medication at least from two weeks before the MRI scans. Supporting Information Table 2 shows the demographic profiles of the two groups. The data was collected from the National Institute of Mental Health-supported project entitled "Neurobiology and Adverse Outcomes of Neuroticism in Late-life Depression" (1R01MH096725). The detailed recruitment criteria have been described elsewhere [Steffens et al., 2015] and in Supporting Information. Diffusion tensor imaging (DTI) data was acquired from a 3.0-Tesla Siemen's Skyra scanner from Olin Neuropsychological Research Center (ONRC) with the following parameters: $B_0 = 1{,}000$ s/mm^2, flip angle = 90°, TR/TE = 17,000 ms/78 ms, imaging matrix = 128 × 128, FOV = 256 × 256 mm^2, 72 contiguous slices, resulting in a voxel dimension of 2 × 2 × 2 mm^3 reconstructed resolution. A total of 128-direction images were acquired. Data preprocessing and analyses on between-hemisphere connectivity as well as its correlation with clinical profiles were the same as described earlier.

RESULTS

There were no significant differences in age, gender, education, or cognitive function between the patient and control groups (Table I). The RGD group had significantly higher depression severity than the control group measured by MADRS (Table I). We did not find a significant change in cognitive function in any specific domain over the 1 year follow up in the RGD group compared with the control group (Supporting Information Table 3).

Alterations in the Between-Hemisphere Connectivity Strength

There was significantly reduced between-hemisphere connectivity in geriatric depression compared with healthy controls using both the low and high resolution analyses (Fig. 2 and Supporting Information Fig. 1). We further investigated whether the reduced between-hemisphere connectivity strength had any relationship with clinical measures. We did not find a significant correlation neither with depression severity nor with the number of depression episodes. However, since the relationship may not be linear, we further regrouped the RGD patients into two subgroups based on the number of depressive episodes, comparing those with two or fewer episodes ($n = 12$) and those with greater than two episodes ($n = 10$). Two subjects did not have the number of depression episodes recorded and were not included in this analysis. A Student t-test was computed to examine whether there were significant differences between the two groups. We found that the multiple episodes group had a significant reduction in the between-hemisphere connectivity strength compared with the few episodes group (Fig. 2) in both low resolution network ($P = 0.019$) and high resolution network analysis ($P = 0.0142$) (Supporting Information Fig. 1). Further analysis on the association of decreased between-hemisphere connectivity and MADRS score increase over the 1 year follow up was not significant. We then grouped subjects into high and low between-hemisphere connectivity strength using median split and found no significant difference between the two groups in terms of the possibility of developing a new episode in the following year.

As shown in Supporting Information Figure 2 from the replication dataset with DTI of 128 directions, we confirmed that the currently depressed patient group also showed reduced between-hemisphere connectivity compared with the control group. Given the fact that in this depressed dataset, the majority of patients had two or fewer episodes of depression, we were not able to conduct correlation analysis with depression episodes or dividing the patient group by depression episodes of two and over versus those with depression episodes of less than two. We then regrouped the depressed patients by duration of current episode using the median split and we found that patients with longer duration had significantly lower between-hemisphere connectivity than those with shorter duration ($P = 0.04$).

Alterations in Hub Distribution and NBS Analysis in RGD Patients

Hub distribution

We computed the hub regions for each group. As shown in Figure 3, there were 14 hubs in the control group (Fig. 3a) and 16 hubs in the RGD group (Fig. 3b). The detailed hubs are listed in Table II. As shown in Table II, thirteen

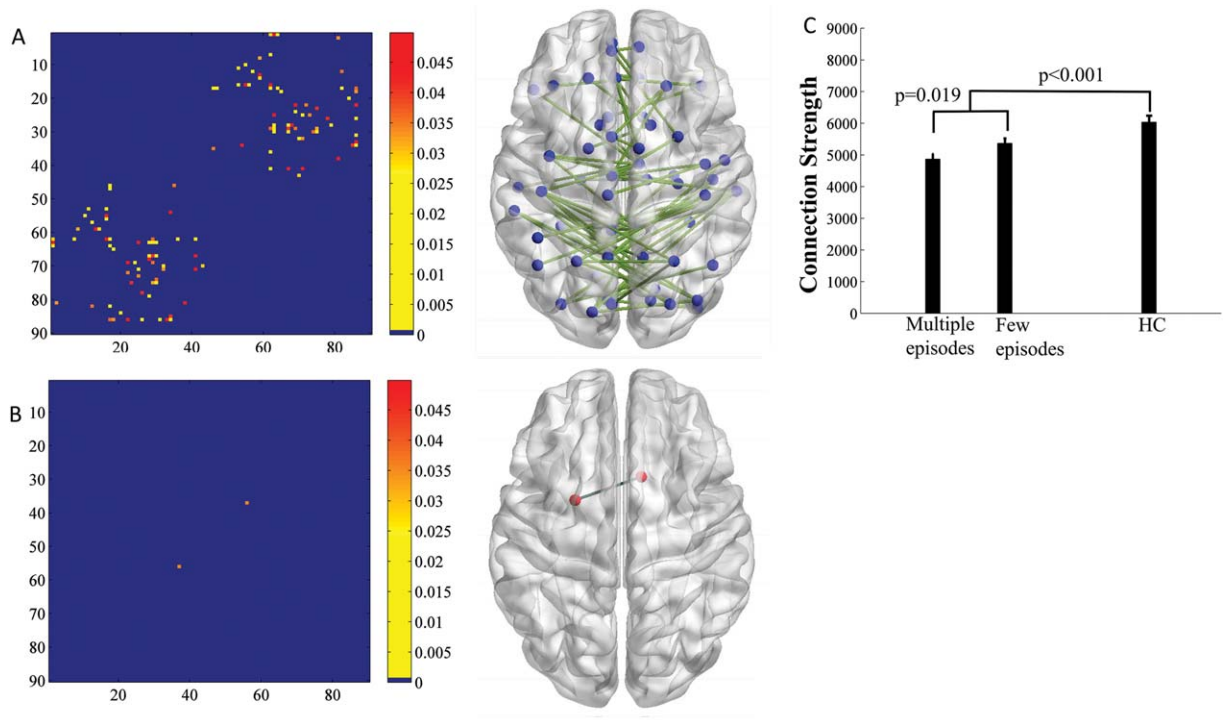

Figure 2.

Comparison of the between-hemisphere connectivity strength (number of edges) between the RGD and healthy control groups. **A**, edges that showed a significant reduction in between-hemisphere connectivity in the RGD group relative to the control group. **B,** Edges that showed a significant increase in between-hemisphere connectivity in the RGD group relative to the control group. The color bars represent significant level of statistics. The nodal regions out of the 90 nodes are constructed according to their centroid stereotaxic coordinates. **C,** Bar graph indicating that the RGD patients who had multiple depression episodes (>2, Multiple Episodes) had significantly lower strength in between-hemisphere connectivity than patients who had a few depression episodes (<2, Few Episodes) and healthy controls in low resolution network analysis. [Color figure can be viewed at wileyonlinelibrary.com.]

out of the 14 hubs were identical for the two groups, including the bilateral dorsal and medial superior frontal gyrus, middle frontal gyrus (MFG), precentral gyrus (PreCG), postcentral gyrus (PoCG), precuneus (PCUN), and right calcarine fissure and surrounding cortex (CAL.R). Three hub regions including the left Inferior temporal gyrus (ITG.L), calcarine fissure and surrounding cortex (CAL.L), and middle temporal gyrus (MTG.L) were identified as hubs in the RGD group, but not in the control group, whereas the right supplementary motor area (SMA.R) was identified as a hub in the control group, but not in the RGD group.

Alterations in NBS analysis

Using NBS analysis, we found a decreased subnetwork (Fig. 4) primarily involving the left lingual gyrus, left middle occipital gyrus, and left fusiform gyrus. The strength of this subnetwork had a positive correlation with information processing speed ($r = 0.47$, $P = 0.0209$) in the RGD group. Similar results were found in the high resolution analysis (Supporting Information Fig. 3).

Alterations in Global and Regional Network Properties of the RGD Group

Alterations in the global properties of WM networks in RGD patients

Compared with controls, the global clustering coefficient was significantly decreased in the RGD group ($t = -1.71$, $P = 0.047$) (Fig. 5). In addition, in the RGD group, information processing speed was significantly correlated with the network properties of global efficiency ($r = 0.37$, $P = 0.0094$), global fault tolerant efficiency ($r = 0.36$, $P = 0.0112$), global network strength ($r = 0.38$, $P = 0.0073$), and negatively correlated with shortest path length ($r = -0.39$, $P = 0.0067$) (Fig. 5). All of the correlations passed the FDR correction with $q < 0.5$. Similar findings were not found in the healthy control group.

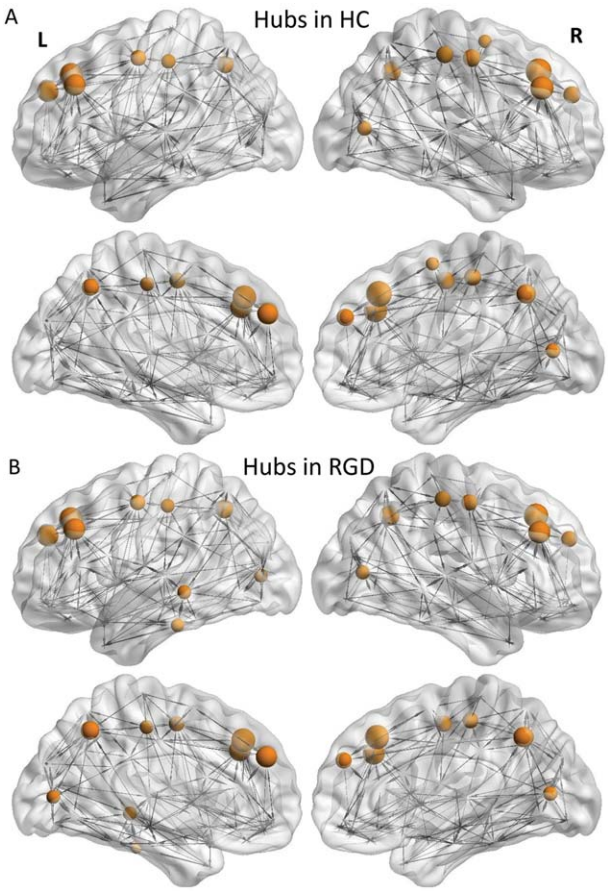

Figure 3.
Distribution of hubs in the WM structural networks of (A) the control group, and (B) the RGD group. [Color figure can be viewed at wileyonline library.com.]

Alterations in the regional properties of WM networks in patients

Regarding the analyses on regional properties, as shown in Figure 6, there were differences between RGD and control groups in a number of regions including middle temporal gyrus, left lingual gyrus, left supramarginal gyrus, right superior frontal gyrus, right supplementary motor area, right inferior occipital gyrus, right superior temporal gyrus, and right inferior temporal gyrus with $P < 0.05$. The nodal efficiency and network strength were decreased, and the shortest path length was significantly increased in remitted patients compared with controls in these nodes. Those regions that at least two network measures with $P < 0.05$ were shown in Figure 6. Although these regions did not pass the FDR correction for multiple comparisons, the network properties across these regions were significantly correlated with cognitive function. Memory performance was positively correlated with the averaged nodal clustering coefficient ($r = 0.47$, $P = 0.0192$) across these regions, and the information processing speed was positively correlated with averaged regional global efficiency ($r = 0.46$, $P = 0.0228$), and network strength ($r = 0.47$, $P = 0.021$) (Fig. 6). All the correlations passed the FDR correction for multiple comparisons with $q < 0.05$.

Neither the global nor the regional network property measures showed any correlations with depression severity or depression episodes.

Instability of the Networks in Depressed Patients in the 1-Year Follow Up

Global efficiency, global fault tolerant efficiency, and global network strength were significantly decreased, and the shortest path length was significantly increased in remitted patients over the 1-year follow up period (Supporting Information Fig. 4). For further details, see Supporting Information.

DISCUSSION

In this study, we examined the microstructural white matter deficits in geriatric depression patients using between-hemisphere connectivity, NBS, and graph theoretical measures. These patients were not currently depressed at the time of baseline MRI scan. We found significantly reduced between-hemisphere connectivity in patients relative to the healthy controls, and that those with greater number of lifetime depression episodes had stronger reduction in between-hemisphere connectivity than those

TABLE II. Hub regions of WM networks in RGD and control groups

RGD (mean = 181.24)			Control (mean = 190.63)		
ID	Hub regions	E_node/ mean	ID	Hub regions	E_node/ mean
1	PreCG.L	1.17	1	PreCG.L	1.2
2	SFGdor.L	1.8	2	SFGdor.L	1.78
4	MFG.L	1.65	4	MFG.L	1.63
12	SFGmed.L	1.63	12	SFGmed.L	1.6
29	PoCG.L	1.06	29	PoCG.L	1.09
34	PCUN.L	1.42	34	PCUN.L	1.29
46	PreCG.R	1.23	46	PreCG.R	1.33
47	SFGdor.R	1.84	47	SFGdor.R	1.95
49	MFG.R	1.67	49	MFG.R	1.75
57	SFGmed.R	1.23	57	SFGmed.R	1.3
67	CAL.R	1.1	67	CAL.R	1.13
74	PoCG.R	1.2	74	PoCG.R	1.28
79	PCUN.R	1.53	79	PCUN.R	1.46
22	CAL.L	1.04	55	SMA.R	1.01
43	MTG.L	1.06			
45	ITG.L	1.01			

The hub regions were identified if node efficiency (E_node) was at least 1 SD greater than the mean node efficiency [i.e., E_node(i)>mean + SD].

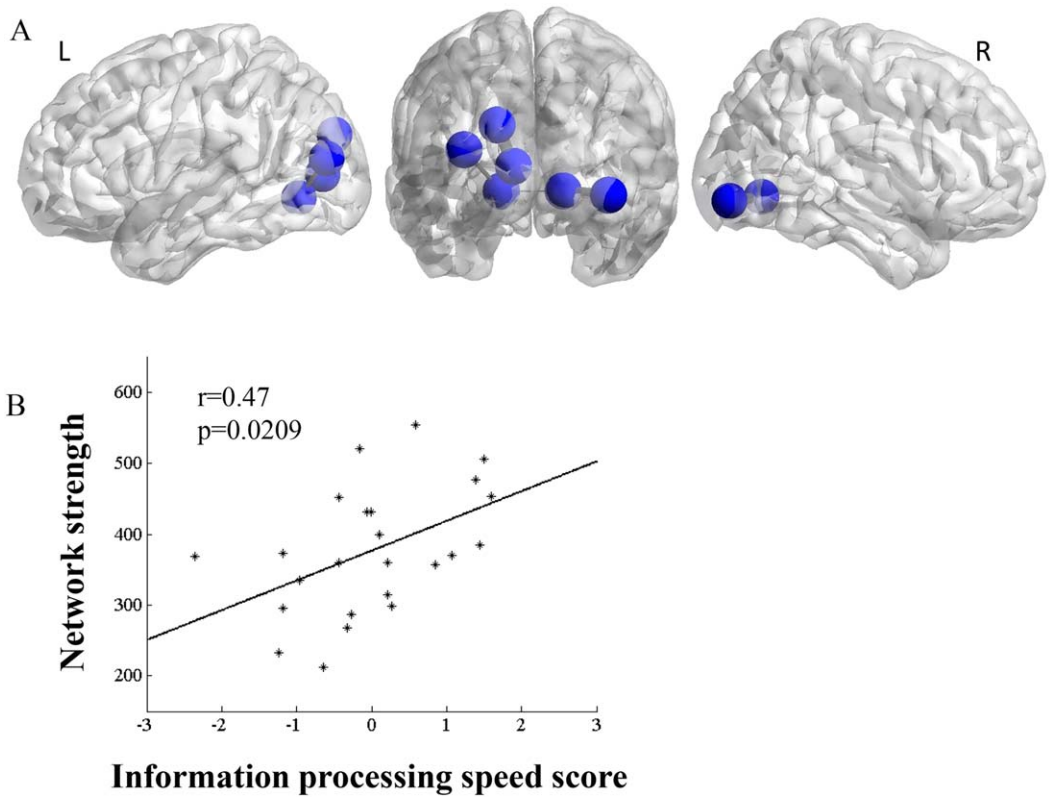

Figure 4.

(A) Comparison of the regions that showed significantly decreased white matter connection in RGD patients relative to the controls (NBS for multiple comparison correction) using 90 nodes to construct networks. Analyses exhibited significantly reduced white matter connection in the temporal and occipital regions. (B) Lower network strength in the RGD group was associated with poorer performance in information processing speed. [Color figure can be viewed at wileyonlinelibrary.com.]

with a fewer depressive episodes. The global and regional network properties were attenuated in the depression group as well. The altered graph network properties were correlated with cognitive dysfunction, but not with depression severity or the number of depressive episodes. In addition, global and local network properties altered greatly in the depression group in the 1-year follow-up scan, suggesting instability of the white matter network connectivity in geriatric depression, which could be a marker for subsequent cognitive decline.

The left and right hemisphere functional asymmetry in major depression has been well documented. Hyperfunction of the right prefrontal cortex and hypo-function of the left prefrontal cortex has been found in a number of studies in major depression [Bermpohl et al., 2006; Davidson et al., 2003; Grimm et al., 2008; Keedwell et al., 2005; Mayberg, 2003]. Here, we showed the reduced between-hemisphere connectivity using DTI in geriatric depression patients who were at the remitted state, which could explain the functional asymmetry between the left and right hemisphere. Future studies in resting-state and task-related fMRI are necessary to confirm whether the reduced between-hemisphere structural connectivity is related to frontal asymmetric function in major depression. Nusslock et al. [2011] found that asymmetric frontal activity prospectively predicted onset of first depressive episode. Given that white matter hyperintensity has been associated with geriatric depression, we speculated that the between-hemisphere connectivity reduction could predict the recurrence of future depressive episodes. However, when grouping subjects into high and low between-hemisphere connectivity strength (using median split), there was no significant difference between the two groups in terms of the possibility of developing a new episode in the following year. This might be due to the fact that 1-year observation was too short for the recurrence of a new depressive episode. Longer-term follow-up studies in a larger sample size are needed in the future to verify if the between-hemisphere connectivity could have prediction value for future depressive episodes. Although we did not find a

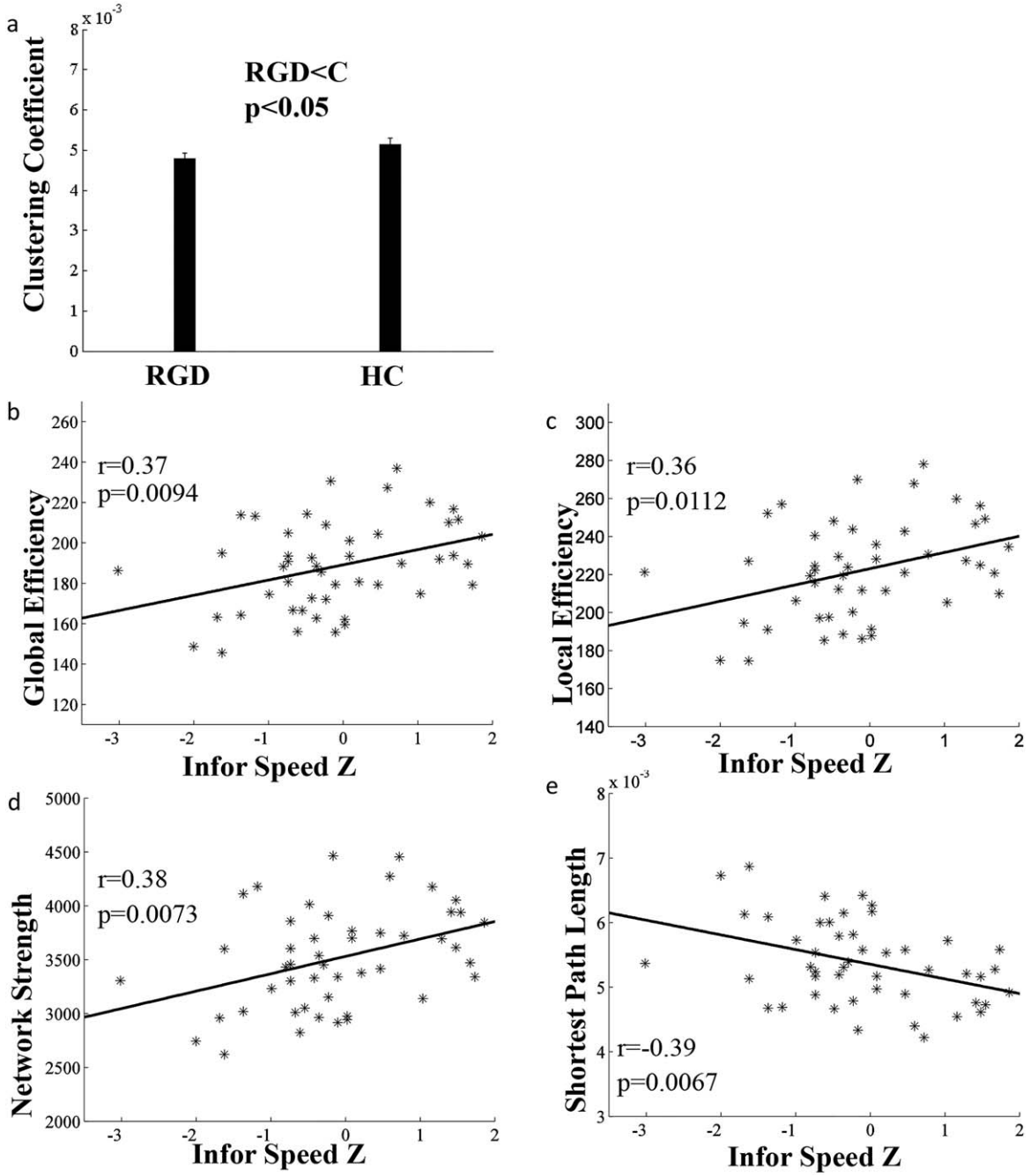

Figure 5.

Significant difference in global network properties between the RGD and healthy control groups (HC). **(a)** Compared with the healthy controls, the RGD group had significantly decreased global clustering coefficient; (**b, f, d**) Lower global efficiency, local efficiency and network strength were associated with poorer performance in information processing speed; (**e**) Longer shortest path length was correlated with poorer performance in information processing speed.

direct link between decreased between-hemisphere connectivity with depression recurrence, we did find a significantly stronger reduction in between-hemisphere connectivity in patients with greater number of depressive episodes. This result suggests a possibility of bidirectional influence between depressive episodes and microstructural damages.

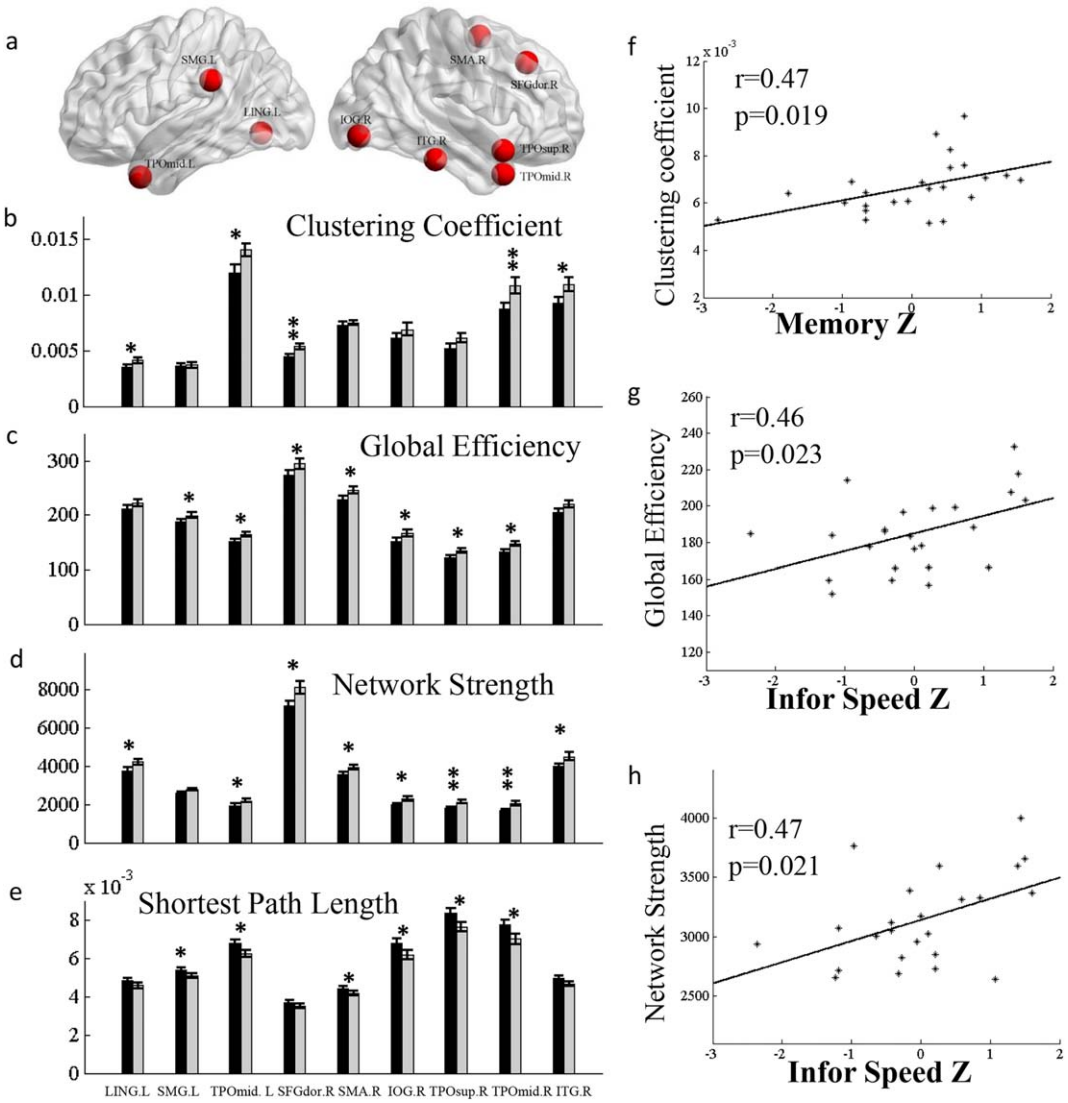

Figure 6.

(a) Nodes that showed significantly reduced regional network properties in the RGD patients relative to controls. Only the regions that had significant reduction in at least two out of the four regional network measures, that is, **(b)** clustering coefficient, **(c)** global efficiency, **(d)** network strength, and **(e)** shortest path length were included here. * indicates a significant group difference at $P < 0.05$, ** indicates a significant group difference at $P < 0.01$. LING.L, left lingual gyrus, SMG.L, left supramarginal gyrus, TPOmid.L, left middle temporal gyrus, SFGdor.R, right dorsal portion of the superior frontal gyrus, SMA.R, right supplementary motor area, IOG.R, right inferior occipital gyrus, TOPsup.R, right superior temporal gyrus, TOPmid.R, right middle temporal gyrus, ITG.R, right inferior temporal gyrus. **(f)** The memory performance in the RGD group had a positive correlation with the averaged clustering coefficient across those regions as listed in **b,c,d,e**. The information processing speed was also positively correlated with **(g)** global efficiency, and **(h)** network strength. [Color figure can be viewed at wileyonlinelibrary.com.]

Given that the number of diffusion-encoding gradient directions might impact on the between-hemisphere connectivity in regions with intensive fibers, we further validated the results using a dataset with 128 directions in a currently depressed group. Consistent with the results in RGD group, we also found the reduction of between-hemisphere connectivity in currently depressed patients relative to healthy controls. Importantly, we also found lower between-hemisphere connectivity in those with a longer duration of current depression episode than those

with a shorter duration, which confirmed that the between-hemisphere was not a depression state effect, rather it was a depression disease accumulation effect.

Notably, this study was conducted in geriatric depression, whereas the frontal asymmetry findings in the literature are mainly from studies in depression among younger adults. Therefore, there is still a gap between the reduced between-hemisphere connectivity reduction and frontal functional asymmetry in geriatric depression. To confirm whether there is asymmetry in frontal functional connectivity in geriatric depression and whether there is reduced between-hemisphere white-matter connectivity in non-geriatric depression, future studies are needed to compare the structural and functional between-hemisphere connectivity in major depression between younger and older adults.

Based on our results of the network-based statistical analysis, the altered subnetwork connectivity in geriatric depression was quite different from the findings in younger depression study but more similar to the findings in the older depression study reported in the literature. In the study by Korgaonkar et al. [2014] in younger depressed patients, significantly lowered structural connectivity within the default mode network and the frontal cortex, thalamus, and caudate were reported, whereas we found significantly reduced white matter connection among the regions in the middle occipital and inferior temporal areas in geriatric depression participants. Bai and colleagues also reported significantly reduced network connection in remitted geriatric depression among many regions including the temporal (superior, middle and inferior temporal gyrus), occipital (superior, middle and inferior occipital gyrus, and fusiform gyrus) as well as limbic and subcortical regions. Therefore, consistent with the literature, our results indicate that there might be etiological differences between younger and older depression.

Unlike the reduced between-hemisphere connectivity results, the reduced global network measures did not have a relationship with the depression episodes. Instead, they were correlated with cognitive dysfunction. Bai and his colleagues' study also had shown reduced clustering coefficient and global efficiency. However, no significant correlation with cognitive function was reported in their study [Bai et al., 2012]. Our results extend previous findings in that the global network measures including the global and local clustering coefficient, global efficiency, and network strength were correlated with cognitive function. Low clustering coefficient was correlated with lower performances in memory information processing speed. Similar findings were found in a functional network study in depression and in a structural network study in MCI and Alzheimer's disease [Ajilore et al., 2014; Bai et al., 2012; Lo et al., 2010]. These findings are also consistent with previous findings that the global network properties are associated with IQ [Fischer et al., 2014; Li et al., 2009], suggesting that the global network measures could be used for evaluating cognitive dysfunction across a number of clinical conditions.

Similar to the global network properties, changes in the regional network measures in the bilateral middle temporal gyrus, left lingual gyrus, left supramarginal gyrus, right dorsal superior frontal gyrus, right supplementary motor area, right inferior occipital gyrus, right superior temporal gyrus, and right inferior temporal gyrus were correlated with cognitive function. The involvement of these prefrontal, temporal, and occipital regions in attention, executive function, and visual memory have been well documented [Alexopoulos et al., 2002; Dalby et al., 2010; Murphy et al., 2007; Sheline et al., 2008]. Therefore, it is not surprising that the network properties in these regions were associated with memory and information processing speed. Our findings indicate that the white matter network deficits in these regions could explain the frequently occurring cognitive dysfunction in geriatric depression.

We used the high resolution analysis to verify our results. The analysis on the between-hemisphere connectivity showed similar results as the low resolution analyses, but the statistics were more significant. The high resolution analysis on the subnetwork connectivity using NBS analysis showed similar but finer degree. This result is also in consistent with the study of Bai et al. [2012]. Our results indicate that using nodes based on both low and high spatial resolution do not affect results significantly.

Another finding in this study is significant changes of network properties in the RGD group relative to the controls over the 1-year follow-up period. We acknowledge the sample size was too small to draw conclusions in our current study; however, to our knowledge this is the first attempt to address the changes of white matter network properties over time in geriatric depression. Since we found the global and regional network properties were correlated with cognitive function instead of depressive severity or depressive episodes, we speculate that the instability of the global and network properties could be a predispositional factor for cognitive decline in patients with geriatric depression. Future replications of the finding in a larger sample with longer observation period are very necessary to confirm our conclusions.

In addition to relatively small sample size, there are also a number of other limitations of the current study, which include possibility of false positive findings in the graph theory and NBS analyses as well as variability in antidepressant medications in the remitted depression group. We acknowledge that even though our findings had passed the FDR correction for multiple comparisons, there is still a possibility of false positive findings. Therefore, a much larger sample size is needed to validate our findings in the future. Although low white matter integrity has been found associated with poor responses to antidepressants [Aizenstein et al., 2014], evidence of how antidepressants effect on white matter integrity is still lacking. While almost half participants of our remitted depression study were under variety of antidepressant medications, the

currently depressed patients were all free of medication for at least two weeks before the MRI scan. Therefore, we can conclude that the results were less likely to be due to current medication although we could not rule out previous medication effect.

SUMMARY

In summary, we found reduced between-hemisphere connectivity was related to depressive episodes, whereas reduced global or nodal clustering efficiency was correlated with cognitive dysfunction in geriatric depression. Reduced between-hemisphere connectivity was related to the number depressive episodes in a long run, whereas the global and nodal clustering efficiency was unstable, which could be predispositional to cognitive decline. Future confirmation of these results in large sample and comparison with the functional network properties would be very beneficial for identifying imaging markers of depression relapse and cognitive decline in geriatric depression.

REFERENCES

Aizenstein HJ, Khalaf A, Walker SE, Andreescu C (2014): Magnetic resonance imaging predictors of treatment response in late-life depression. J Geriatr Psychiatry Neurol 27:24–32.

Ajilore O, Lamar M, Kumar A (2014): Association of brain network efficiency with aging, depression, and cognition. Am J Geriatr Psychiatry 22:102–110.

Alexopoulos GS, Meyers BS, Young RC, Campbell S, Silbersweig D, Charlson M (1997): 'Vascular depression' hypothesis. Arch Gen Psychiatry 54:915–922.

Alexopoulos GS, Kiosses DN, Klimstra S, Kalayam B, Bruce ML (2002): Clinical presentation of the "depression-executive dysfunction syndrome" of late life. Am J Geriatr Psychiatry 10: 98–106.

Bai F, Shu N, Yuan Y, Shi Y, Yu H, Wu D, Wang J, Xia M, He Y, Zhang Z (2012): Topologically convergent and divergent structural connectivity patterns between patients with remitted geriatric depression and amnestic mild cognitive impairment. J Neurosci 32:4307–4318.

Basser PJ, Pajevic S, Pierpaoli C, Duda J, Aldroubi A (2000): In vivo fiber tractography using DT-MRI data. Magn Reson Med 44:625–632.

Behrens TE, Woolrich MW, Jenkinson M, Johansen-Berg H, Nunes RG, Clare S, Matthews PM, Brady JM, Smith SM (2003): Characterization and propagation of uncertainty in diffusion-weighted MR imaging. Magn Reson Med 50:1077–1088.

Bermpohl F, Fregni F, Boggio PS, Thut G, Northoff G, Otachi PT, Rigonatti SP, Marcolin MA, Pascual-Leone A (2006): Effect of low-frequency transcranial magnetic stimulation on an affective go/no-go task in patients with major depression: Role of stimulation site and depression severity. Psychiatry Res 141: 1–13.

Boccaletti S, Latora V, Moreno Y, Chavez M, Hwang DU (2006): Complex networks: Structure and dynamics. Phys Rep 424: 175–308.

Brown RA, Narayanan S, Arnold DL (2013): Segmentation of magnetization transfer ratio lesions for longitudinal analysis of demyelination and remyelination in multiple sclerosis. NeuroImage 66:103–109.

Bullmore ET, Sporns O (2009): Complex brain networks: Graph theoretical analysis of structural and functional systems. Nat Rev Neurosci 10:186–198.

Cao Q, Shu N, An L, Wang P, Sun L, Xia MR, Wang JH, Gong GL, Zang YF, Wang YF, He Y (2013): Probabilistic diffusion tractography and graph theory analysis reveal abnormal white matter structural connectivity networks in drug-naive boys with attention deficit/hyperactivity disorder. J Neurosci 33: 10676–10687.

Choi KS, Holtzheimer PE, Franco AR, Kelley ME, Dunlop BW, Hu XP, Mayberg HS (2014): Reconciling variable findings of white matter integrity in major depressive disorder. Neuropsychopharmacology 39:1332–1339.

Cohen AL, Fair DA, Dosenbach NUF, Miezin FM, Dierker D, Van Essen DC, Schlaggar BL, Petersen SE (2008): Defining functional areas in individual human brains using resting functional connectivity MRI. NeuroImage 41:45–57.

Dalby RB, Frandsen J, Chakravarty MM, Ahdidan J, Sorensen L, Rosenberg R, Videbech P, Ostergaard L (2010): Depression severity is correlated to the integrity of white matter fiber tracts in late-onset major depression. Psychiatry Res-Neuroimaging 184:38–48.

Davidson RJ (1993): Cerebral asymmetry and emotion: Conceptual and methodological conundrums. Cogn Emotion 7:115–138.

Davidson RJ, Irwin W, Anderle MJ, Kalin NH (2003): The neural substrates of affective processing in depressed patients treated with venlafaxine. Am J Psychiatry 160:64–75.

Drevets WC, Price JL, Furey ML (2008): Brain structural and functional abnormalities in mood disorders: Implications for neurocircuitry models of depression. Brain Struct Funct 213:93–118.

Elliott R, Rubinsztein JS, Sahakian BJ, Dolan RJ (2002): The neural basis of mood-congruent processing biases in depression. Arch Gen Psychiatry 59:597–604.

Fischer FU, Wolf D, Scheurich A, Fellgiebel A (2014): Association of structural global brain network properties with intelligence in normal aging. PloS One 9:e86258.

Gong GL, He Y, Concha L, Lebel C, Gross DW, Evans AC, Beaulieu C (2009a): Mapping anatomical connectivity patterns of human cerebral cortex using in vivo diffusion tensor imaging tractography. Cereb Cortex 19:524–536.

Gong GL, Rosa P, Carbonell F, Chen ZJ, He Y, Evans AC (2009b): Age- and gender-related differences in the cortical anatomical network. J Neurosci 29:15684–15693.

Grimm S, Beck J, Schuepbach D, Hell D, Boesiger P, Bermpohl F, Niehaus L, Boeker H, Northoff G (2008): Imbalance between left and right dorsolateral prefrontal cortex in major depression is linked to negative emotional judgment: An fMRI study in severe major depressive disorder. Biol Psychiatry 63: 369–376.

Hagmann P, Kurant M, Gigandet X, Thiran P, Wedeen VJ, Meuli R, Thiran JP (2007): Mapping human whole-brain structural networks with diffusion mrI. PloS One 2:e597.

Hagmann P, Cammoun L, Gigandet X, Meuli R, Honey CJ, Wedeen V, Sporns O (2008): Mapping the structural core of human cerebral cortex. PLoS Biol 6:1479–1493.

He Y, Chen Z, Evans A (2008): Structural insights into aberrant topological patterns of large-scale cortical networks in Alzheimer's disease. J Neurosci 28:4756–4766.

Iturria-Medina Y, Canales-Rodriguez EJ, Melie-Garcia L, Valdes-Hernandez PA, Martinez-Montes E, Aleman-Gomez Y, Sanchez-Bornot JM (2007): Characterizing brain anatomical connections using diffusion weighted MRI and graph theory. NeuroImage 36:645–660.

Iturria-Medina Y, Sotero RC, Canales-Rodriguez EJ, Aleman-Gomez Y, Melie-Garcia L (2008): Studying the human brain anatomical network via diffusion-weighted MRI and Graph Theory. NeuroImage 40:1064–1076.

Johansen-Berg H, Behrens TEJ, Robson MD, I,D, Rushworth MFS, Brady JM, Smith SM Higham DJ, Matthews PM, (2004): Changes in connectivity profiles define functionally distinct regions in human medial frontal cortex. Proc Natl Acad Sci U S A 101:13335–13340.

Keedwell PA, Andrew C, Williams SCR, Brammer MJ, Phillips ML (2005): The neural correlates of anhedonia in major depressive disorder. Biol Psychiatry 58:843–853.

Korgaonkar MS, Fornito A, Williams LM, Grieve SM (2014): Abnormal structural networks characterize major depressive disorder: A connectome analysis. Biol Psychiatry 76:567–574.

Latora V, Marchiori M (2001): Efficient behavior of small-world networks. Phys Rev Lett 87:198701.

Li Y, Liu Y, Li J, Qin W, Li K, Yu C, Jiang T (2009): Brain anatomical network and intelligence. PLoS Comput Biol 5:e1000395.

Li H, Xue Z, Ellmore TM, Frye RE, Wong ST (2014): Network-based analysis reveals stronger local diffusion-based connectivity and different correlations with oral language skills in brains of children with high functioning autism spectrum disorders. Hum Brain Mapp 35:396–413.

Lo CY, Wang PN, Chou KH, Wang JH, He Y, Lin CP (2010): Diffusion tensor tractography reveals abnormal topological organization in structural cortical networks in Alzheimer's disease. J Neurosci 30:16876–16885.

Maeda F, Keenan JP, Tormos JM, Topka H, Pascual-Leone A (2000): Modulation of corticospinal excitability by repetitive transcranial magnetic stimulation. Clin Neurophysiol 111:800.

Mayberg HS (2003): Modulating dysfunctional limbic-cortical circuits in depression: Towards development of brain-based algorithms for diagnosis and optimised treatment. Br Med Bull 65: 193–207.

Mayberg HS (2009): Targeted electrode-based modulation of neural circuits for depression. J Clin Invest 119:717–725.

Murphy CF, Gunning-Dixon FM, Hoptman MJ, Lim KO, Ardekani B, Shields JK, Hrabe J, Kanellopoulos D, Shanmugham BR, Alexopoulos GS (2007): White-matter integrity predicts stroop performance in patients with geriatric depression. Biol Psychiatry 61:1007–1010.

Nusslock R, Shackman AJ, Harmon-Jones E, Alloy LB, Coan JA, Abramson LY (2011): Cognitive vulnerability and frontal brain asymmetry: Common predictors of first prospective depressive episode. J Abnorm Psychol 120:497–503.

Petrella JR (2011): Use of graph theory to evaluate brain networks: A clinical tool for a small world? Radiology 259:317–320.

Phillips ML (2003): Understanding the neurobiology of emotion perception: Implications for psychiatry. Br J Psychiatry 182: 190–192.

Robins LN, Helzer JE, Croughan J, Ratcliff KS (1981): National institute of mental health diagnostic interview schedule. Its history, characteristics, and validity. Arch Gen Psychiatry 38:381–389.

Sackeim HA, Greenberg MS, Weiman AL, Gur RC, Hungerbuhler JP, Geschwind N (1982): Hemispheric-asymmetry in the expression of positive and negative emotions - neurologic evidence. Arch Neurol 39:210–218.

Sheline YI, Price JL, Vaishnavi SN, Mintun MA, Barch DM, Epstein AA, Wilkins CH, Snyder AZ, Couture L (2008): Regional white matter hyperintensity burden in automated segmentation distinguishes late-life depressed subjects from comparison subjects matched for vascular risk factors. Am J Psychiatry 165:524–532.

Shu N, Liu Y, Li KC, Duan YY, Wang J, Yu CS, Dong HQ, Ye J, He Y (2011): Diffusion tensor tractography reveals disrupted topological efficiency in white matter structural networks in multiple sclerosis. Cereb Cortex 21:2565–2577.

Smith SM, Jenkinson M, Woolrich MW, Beckmann CF, Behrens TEJ, Johansen-Berg H, Bannister PR, De Luca M, Drobnjak I, Flitney DE, Niazy RK, Saunders J, Vickers J, Zhang YY, De Stefano N, Brady JM, Matthews PM (2004): Advances in functional and structural MR image analysis and implementation as FSL. NeuroImage 23:S208–S219.

Steffens DC, Taylor WD, Denny KL, Bergman SR, Wang LH (2011): Structural integrity of the uncinate fasciculus and resting state functional connectivity of the ventral prefrontal cortex in late life depression. PloS One 6:e22697.

Steffens DC, Manning KJ, Wu R, Grady JJ, Fortinsky RH, Tennen HA (2015): Methodology and preliminary results from the neurobiology of late-life depression study. Int Psychogeriatr 27: 1987–1997.

Taylor S (2013): Molecular genetics of obsessive-compulsive disorder: A comprehensive meta-analysis of genetic association studies. Mol Psychiatry 18:799–805.

Tzourio-Mazoyer N, Landeau B, Papathanassiou D, Crivello F, Etard O, Delcroix N, Mazoyer B, Joliot M (2002): Automated anatomical labeling of activations in SPM using a macroscopic anatomical parcellation of the MNI MRI single-subject brain. NeuroImage 15:273–289.

Wang L, Xia M, Li K, Zeng Y, Su Y, Dai W, Zhang Q, Jin Z, Mitchell PB, Yu X, He Y, Si T (2015): The effects of antidepressant treatment on resting-state functional brain networks in patients with major depressive disorder. Hum Brain Mapp 36:768–778.

Watts DJ, Strogatz SH (1998): Collective dynamics of 'small-world' networks. Nature 393:440–442.

Wei Q, Tian Y, Yu Y, Zhang F, Hu X, Dong Y, Chen Y, Hu P, Hu X, Wang K (2014): Modulation of interhemispheric functional coordination in electroconvulsive therapy for depression. Transl Psychiatry 4:e453.

Yap PT, Wu GR, Shen DG (2010): Human brain connectomics: Networks, techniques, and applications. IEEE Signal Proc Mag 27:131–134.

Zalesky A, Fornito A, Bullmore ET (2010a): Network-based statistic: Identifying differences in brain networks. NeuroImage 53: 1197–1207.

Zalesky A, Fornito A, Harding IH, Cocchi L, Yucel M, Pantelis C, Bullmore ET (2010b): Whole-brain anatomical networks: Does the choice of nodes matter? NeuroImage 50:970–983.

Zalesky A, Fornito A, Seal ML, Cocchi L, Westin CF, Bullmore ET, Egan GF, Pantelis C (2011): Disrupted axonal fiber connectivity in schizophrenia. Biol Psychiatry 69:80–89.